



HAL
open science

Monitoring the Ratio of Two Normal Variables and Compositional Data: A Literature Review and Perspective

Thi Thuy van Nguyen, Thi Hien Nguyen, Kim Duc Tran, Cédric Heuchenne,
Kim Phuc Tran

► **To cite this version:**

Thi Thuy van Nguyen, Thi Hien Nguyen, Kim Duc Tran, Cédric Heuchenne, Kim Phuc Tran. Monitoring the Ratio of Two Normal Variables and Compositional Data: A Literature Review and Perspective. 2023. hal-04331557

HAL Id: hal-04331557

<https://hal.science/hal-04331557v1>

Preprint submitted on 8 Dec 2023

HAL is a multi-disciplinary open access archive for the deposit and dissemination of scientific research documents, whether they are published or not. The documents may come from teaching and research institutions in France or abroad, or from public or private research centers.

L'archive ouverte pluridisciplinaire **HAL**, est destinée au dépôt et à la diffusion de documents scientifiques de niveau recherche, publiés ou non, émanant des établissements d'enseignement et de recherche français ou étrangers, des laboratoires publics ou privés.

Monitoring the Ratio of Two Normal Variables and Compositional Data: A Literature Review and Perspective

Thi Thuy Van Nguyen^{1,*}, Thi Hien Nguyen², Kim Duc Tran³, Cédric Heuchenne¹ and Kim Phuc Tran⁴

¹HEC Liège - Management School, University of Liège, Belgium

²Laboratoire AGM, UMR CNRS 8088, CY Cergy Paris University, France

³IAD, Dong A University, Da Nang, Vietnam

⁴ENSAIT, GEMTEX, University of Lille, France

Abstract

The ratio of two normal variables and compositional Data (CoDa) are two common types of process data in industrial and manufacturing applications. Control charts are powerful tools in statistical process control for monitoring these types of data, as they allow for the detection of process changes and improvement in process quality. In this chapter, we provide a comprehensive analysis of the existing literature on control charts for monitoring the ratio of two normal variables and CoDa and offer a perspective on the strengths and limitations of these methods, as well as potential areas for future research. Specifically, the review is organized into two main categories: control charts for monitoring the ratio of two normal variables and control charts for monitoring CoDa. In this comprehensive analysis, we examine 87 research studies, comprising 68 that focus on the ratio of two normal variables and 19 that delve into CoDa. This extensive review aims to furnish crucial insights into the application of control charts for monitoring these distinct data types. Moreover, it offers practical recommendations for practitioners on choosing suitable methods and incorporating machine learning techniques to enhance monitoring efficiency. This guidance is particularly pertinent for monitoring industrial processes within the context of Industry 5.0, reflecting the evolving needs and complexities of modern manufacturing environments.

Keywords: Control chart, Ratio, Compositional data, EWMA, CUSUM, Shewhart, Measurement errors, VSI, Statistical process control.

*Corresponding author. Email: ttv.nguyen@uliege.be

Contents

1	Introduction	3
2	The Ratio Control Charts	4
2.1	Derivation of properties of the ratio distribution	4
2.2	Various types of ratio control charts and their descriptions.	8
2.2.1	Shewhart-RZ charts	8
2.2.2	Synthetic RZ-charts	9
2.2.3	Runs Rules RZ charts	9
2.2.4	EWMA RZ charts	10
2.2.5	CUSUM-RZ charts	11
2.3	Adaptive control charts types of ratio	12
2.4	RZ - control charts under the effect of measurement errors	12
3	Monitoring the Compositional Data	13
3.1	Modelling of Compositional Data	13
3.2	Control charts for monitoring CoDa	16
3.2.1	Chi-square control chart	16
3.2.2	Shewhart-type control charts	17
3.2.3	Memory-type control charts	17
3.2.4	Adaptive control charts	19
3.2.5	Control charts under the effect of measurement error or autocorrelation between samples	20
3.3	Analysis	21
4	Perspectives for Monitoring the Ratio of Two Normal Variables and Compositional Data in the Industry 5.0	24
4.1	Intergrating ML techniques in designing control charts	26
4.2	ML-based control charts pattern recognition for monitoring CoDa/Ratio	27
4.3	Interpreting out-of-control signal for CoDa control charts	28
5	Conclusion	29

Acronyms

CoDa	Compositional data
FSI	fixed sampling interval
FSS	Fixed sample size
ML	Machine Learning
MCUSUM	Multivariate cumulative sum
MEWMA	Multivariate exponentially weighted moving average
SPC	Statistical process control
SVDD	Support vector data description
SVM	Support vector machine
UCL	Upper control limit
VSI	Variable sampling interval
VSS	Variable sample size

1 Introduction

In the evolving landscape of manufacturing, marked by the advent of Industry 5.0, the role of control charts in quality monitoring has become increasingly significant. Industry 5.0, characterized by a strong focus on personalization, sustainability, and the synergistic collaboration between humans and technology, demands innovative approaches in quality control to match its complex and dynamic nature. In this context, control charts, a fundamental tool in statistical process monitoring (SPC), are adapting to meet the nuanced needs of this new industrial era.

Control charts are efficient tools in providing a graphical representation of process data, essential for detecting changes in manufacturing processes. Implementing control charts allows manufacturing companies to monitor the quality of their products, thereby reducing waste, preventing defects, and improving production process efficiency. In Industry 5.0, where the manufacturing processes are more intricate and tailored, the need for precise and adaptable quality monitoring tools is paramount. Control charts for monitoring the ratio of two normal random variables and Compositional Data (CoDa) have already received attention and continue to be an important point in this advanced manufacturing paradigm. The ratio of two normal random variables, a common measurement in numerous industrial applications, plays a critical role in ensuring process consistency and detecting production anomalies. This is especially relevant in Industry 5.0, where even minor variations in ratios, such as ingredient proportions in the food industry or dimensional ratios in manufacturing, can significantly impact the final product's quality and customization. CoDa, on the other hand, refers to data representing the proportions of different components that constitute a whole. CoDa is commonly encountered in various industrial applications, such as chemical research, econometrics, and food industries. The control chart for monitoring CoDa is used to monitor the proportions of the different components and detect any changes in their distribution. In the context of Industry 5.0, the control chart for monitoring CoDa becomes crucial for maintaining the integrity of products where the balance of components is key to quality and customer satisfaction. To obtain additional examples of the applications of the ratio of random variables and CoDa, refer to the works of Celano et al.¹ and Aitchison², respectively. While the ratio of two normal variables and CoDa represent distinct types of data, they both fundamentally involve ratios or proportions of different components or variables and share a common aspect of incorporating relative information between them. Specifically, when CoDa is limited to two components and follows a normal distribution within the simplex space, it may exhibit similarities to the ratio of two normal variables (even though they are still fundamentally different due to the constraints on CoDa). Given this shared conceptual foundation in the representation of relative information through ratios or proportions, our review strategically groups control charts designed for monitoring these two

data types.

Consequently, in this chapter, we will provide a comprehensive overview of control charts for monitoring the ratio of two normal random variables and CoDa and provide intuitive outlines for papers in these fields. To achieve this, a comprehensive overview encompassing 87 studies was conducted to identify relevant studies for inclusion in this review. A total of 87 studies were selected based on their relevance, with 68 studies focusing on control charts for monitoring the ratio of two normal random variables and the remaining 19 studies focusing on control charts for monitoring CoDa. To facilitate the analysis and presentation of the selected studies, they were categorized based on data type into two groups: control charts for monitoring the ratio of two normal random variables and control charts for monitoring CoDa. The remainder of the paper is organized as follows: Sections 2 and 3 provide concerns about the control chart for monitoring the ratio of two normal variables and CoDa, together with some discussions on the advantages and disadvantages of these control charts. Section 4 offers some perspective views on the machine learning techniques in the stages of designing, pattern recognition, and interpreting control charts for monitoring Compositional Data (CoDa) and the ratio of two normal random variables, enhancing the understanding of these essential tools in the context of Industry 5.0. Finally, the chapter ends with a summary of the contributions.

2 The Ratio Control Charts

In all production processes, the practitioners must monitor how well their products meet specifications. In more general terms, product quality has two “enemies”: (1) deviations from target product specifications and (2) excessive dispersion around the target product specifications. During the early stages of the development of a production process, the design of experiments is often used to optimize these two quality characteristics, and control charts are effective tools in Statistical Process Control (SPC) for monitoring the stability of a process over time. Currently, most competitive manufacturing companies are implementing SPC in various applications: biology, genetics, medicine, finance, and other areas (see Montgomery³). The design and implementation of control charts monitoring the ratio of two variables are attractive from both theoretical and practical points of view. According to the data from *Web of Science*, interest in this type of chart has increased dramatically in recent years. In fact, Figure 1 shows the revolution of the number of publications and number of citations on the Ratio control charts. A large part of which is *article* published in journals (89.71%), see Table 1 and is in the field of Engineering Industrial (28%) and Operations Research Management Science (26%) (see Fig. 2). Two selection criteria are used to choose and accept the Ratio control chart research articles: 1) papers are found via a computerized search of the topic areas (Quality control, SPC). The search is narrowed using the following terms: Ratio control chart, ratio distribution, and monitoring Ratio. This research considers the published research, including electronic literature sources such as Wiley, Taylor & Francis, Elsevier, Springer Nature, Scopus, etc. Table 2 lists the number of published papers among 36 journals. *Quality and Reliability Engineering International* is ranked first (20 publications and $\sim 29.41\%$) in this area.

In this section, a brief review of the sample distribution of the ratio of two normal variables is recalled. Then, we summarize the differences between the various types of ratio charts and their performances.

2.1 Derivation of properties of the ratio distribution

Suppose that X and Y be the two normal random variables such that $\mathbf{W} = (X, Y)^T \sim N(\boldsymbol{\mu}_{\mathbf{W}}, \boldsymbol{\Sigma}_{\mathbf{W}})$, i.e. \mathbf{W} is a bi-variate normal random vector with mean vector and variance-covariance matrix as

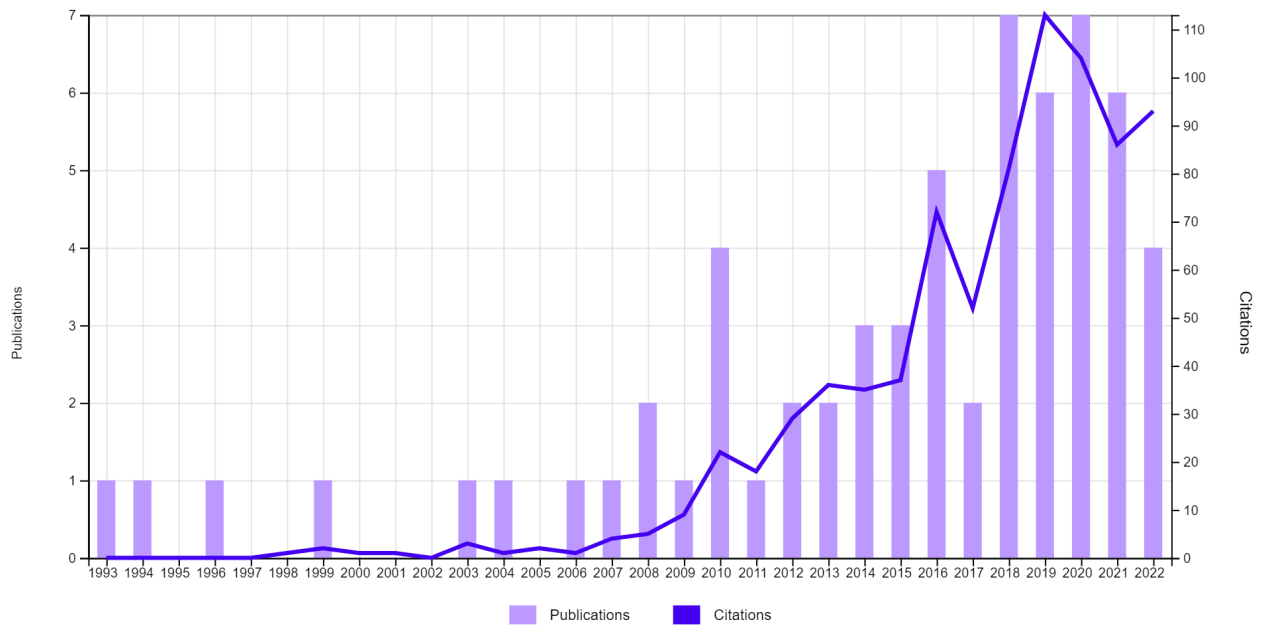


Figure 1: Revolution of publications and citations on Ratio control charts

Document Types	Number	Percentage
Article	61	89.71
Proceeding Paper	4	5.88
Early Access	2	2.94
Letter	1	1.47

Table 1: Document types of publications

Journal name	Number	%
Quality And Reliability Engineering International	20	29.41%
International Journal Of Production Research	4	5.88%
Journal Of Quality Technology	3	4.41%
Communications In Statistics-Theory And Methods	3	4.41%
Journal Of Statistical Computation And Simulation	3	4.41%
Statistical Papers	2	2.94%
Computational Statistics & Data Analysis	2	2.94%
Technometrics	2	2.94%
Computers & Industrial Engineering	2	2.94%
Asqc 48th Annual Quality Congress Proceedings	1	1.47%
American Heart Journal	1	1.47%
Naval Research Logistics	1	1.47%
Journal Of Manufacturing Processes	1	1.47%
International Journal Of Reliability Quality & Safety Engineering	1	1.47%
Scientia Iranica	1	1.47%
Communications In Statistics-Simulation And Computation	1	1.47%
Journal Of Food Science	1	1.47%
Acta Scientiarum-Technology	1	1.47%
Symmetry-Basel	1	1.47%
European Journal Of Operational Research	1	1.47%
Biopharm International	1	1.47%
Arabian Journal For Science And Engineering	1	1.47%
Journal Of Probability And Statistics	1	1.47%
Structural Health Monitoring 2013, Vols 1 And 2	1	1.47%
IIE Transactions	1	1.47%
Engenharia Agricola	1	1.47%
Journal Of Mathematics	1	1.47%
Scientia Iranica Transaction E-Industrial Engineering	1	1.47%
Journal Of Testing And Evaluation	1	1.47%
Quality Innovation Prosperity-Kvalita Inovacia Prosperita	1	1.47%
British Medical Journal	1	1.47%
Science In China Series A-Mathematics	1	1.47%
Productivity & Quality Management Frontiers Iv, Vols 1 And 2	1	1.47%
Journal Of Industrial And Production Engineering	1	1.47%
Icim2012: Proceedings Of The 11th Inter. Conf. On Industrial Management	1	1.47%
Advances And Applications In Statistics	1	1.47%

Table 2: Number and percentage of papers in each journal

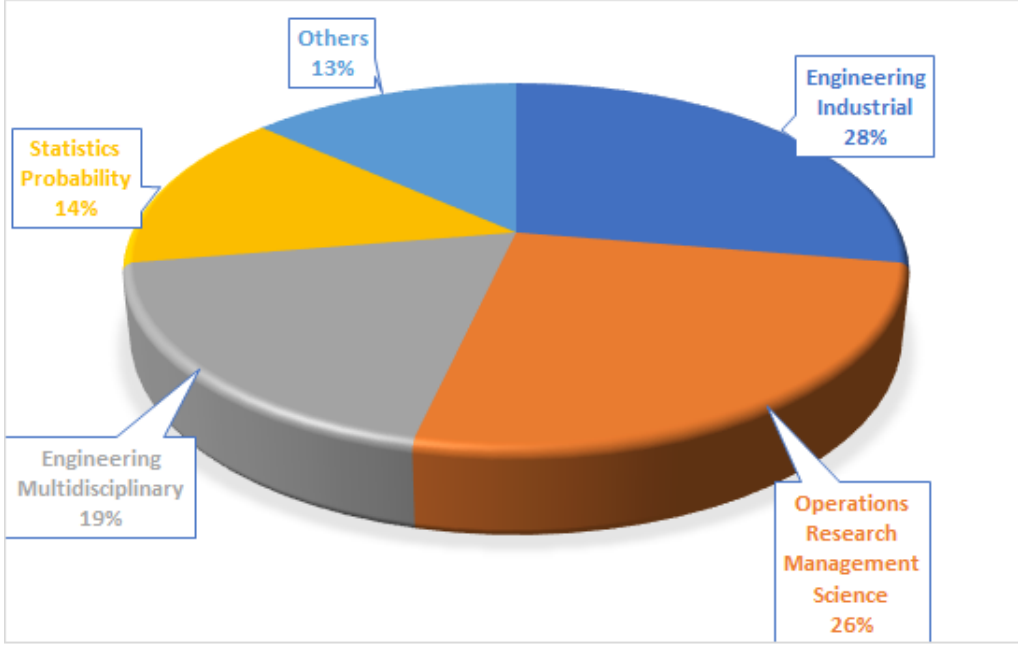


Figure 2: Document types of publications

follows:

$$\boldsymbol{\mu}_{\mathbf{W}} = \begin{pmatrix} \mu_X \\ \mu_Y \end{pmatrix} \quad \text{and} \quad \boldsymbol{\Sigma}_{\mathbf{W}} = \begin{pmatrix} \sigma_X^2 & \rho\sigma_X\sigma_Y \\ \rho\sigma_X\sigma_Y & \sigma_Y^2 \end{pmatrix} \quad (1)$$

where μ_X and μ_Y are the means of two variables and ρ is the correlation coefficient between them. Coefficients of variation (γ_X, γ_Y) and standard-deviation ratio (ω) of X and Y are denoted by $\gamma_X = \frac{\sigma_X}{\mu_X}$, $\gamma_Y = \frac{\sigma_Y}{\mu_Y}$ and $\omega = \frac{\sigma_X}{\sigma_Y}$, respectively. Let Z be the ratio of X to Y ($Z = X/Y$). Celano and Castagliola⁴ derived an adequate approximation for the *c.d.f* (cumulative distribution function) of Z as a function of $\gamma_X, \gamma_Y, \omega$, and ρ as:

$$F_Z(z|\gamma_X, \gamma_Y, \omega, \rho) \simeq \Phi\left(\frac{A}{B}\right), \quad (2)$$

where

$$A = \frac{z}{\gamma_Y} - \frac{\omega}{\gamma_X}, \quad \text{and} \quad B = \sqrt{\omega^2 - 2\rho\omega z + z^2},$$

and Φ is the *c.d.f* of standard normal distribution (Sdn). After some tedious derivations, approximated *p.d.f* (probability density function) of the ratio Z is

$$f_Z(z|\gamma_X, \gamma_Y, \omega, \rho) \simeq \left(\frac{1}{B\gamma_Y} - \frac{(z - \rho\omega)A}{B^3} \right) \times \phi\left(\frac{A}{B}\right), \quad (3)$$

where $\phi(\cdot)$ is the *p.d.f* of Sdn. Solving the equation $F_Z(z|\gamma_X, \gamma_Y, \omega, \rho) = p$ allows obtaining an approximate expression for the *i.d.f* (inverse distribution function) $F_Z^{-1}(p|\gamma_X, \gamma_Y, \omega, \rho)$. We have

$$F_Z^{-1}(p|\gamma_X, \gamma_Y, \omega, \rho) \simeq \begin{cases} \frac{-C_2 - \sqrt{C_2^2 - 4C_1C_3}}{2C_1}, & \text{if } p \in (0, 0.5], \\ \frac{-C_2 + \sqrt{C_2^2 - 4C_1C_3}}{2C_1}, & \text{if } p \in [0.5, 1), \end{cases} \quad (4)$$

where C_1 , C_2 , and C_3 are functions of ω , ρ , γ_X , γ_Y , p and they are:

$$\begin{aligned} C_1 &= \frac{1}{\gamma_Y^2} - (\Phi^{-1}(p))^2, \\ C_2 &= 2\omega \left(\rho (\Phi^{-1}(p))^2 - \frac{1}{\gamma_X \gamma_Y} \right), \\ C_3 &= \omega^2 \left(\frac{1}{\gamma_X^2} - (\Phi^{-1}(p))^2 \right), \end{aligned}$$

and where $\Phi^{-1}(\cdot)$ is the *i.d.f.* of Sdn.

2.2 Various types of ratio control charts and their descriptions.

In the SPC literature, the research on control charts for monitoring the ratio of two normal random distributions is mainly focused on some types of charts: the traditional Shewhart charts that we denote RZ-chart, overcome the problem of the Shewart chart in the case the small shift-size (Synthetic-RZ, Run-Rule RZ, cumulative sum charts (CUSUM -RZ) and the exponentially weighted moving average charts (EWMA-RZ). After that, to improve the performance of these charts, the researchers found some adaptive models. In other studies, they are looking for the effect of measurement errors on the performance of RZ-charts. In this subsection, we make a summary of these types and give some comments.

2.2.1 Shewhart-RZ charts

With this traditional type chart, the first author to mention is Spisak⁵. He investigated a quality control procedure for insurance against unemployment by estimating the bias in a ratio estimator. An illustrative example in his work is the Department of Labor's Unemployment Insurance Quality Control program. Other applications of ratio control charts are also mentioned. Oksoy et al.⁶ discussed some useful guidelines to implement the ratio chart for supervising and controlling the ratio $Z = X/Y$ of glass oxide. Celano et al.¹ design the Shewhart chart based on individual measurements, (i.e. at fixed sampling times k , the sample size is $n = 1$). They are named the Shewhart-RZ control chart. This chart, monitoring the ratio $Z_k = X_k/Y_k$, is designed regarding a couple of probability action limits, upper control limit (UCL) and lower control limit (LCL) as follows

$$\begin{aligned} \text{UCL}_{RZ} &= F_Z^{-1} \left(1 - \frac{\alpha}{2} \mid \gamma_{X_0}, \gamma_{Y_0}, \omega_0, \rho \right) \\ \text{LCL}_{RZ} &= F_Z^{-1} \left(\frac{\alpha}{2} \mid \gamma_{X_0}, \gamma_{Y_0}, \omega_0, \rho \right) \end{aligned}$$

where α is the type I error probability associated with the control chart. The chart issues an out-of-control when $Z_i > \text{UCL}_{RZ}$ or $Z_i < \text{LCL}_{RZ}$. The authors considered an illustrative example in food manufacturing; they check the stability of the ratio Z between the weight of almonds and raisins and the total weight of muesli (a mixture of whole grain, rolled oats, raisins, almonds, and several kinds of seeds). The result of the Shewhart-RZ chart showed that between samples #12 and #13, there is an error report (the process is out of control). Extending this work, Celano and Castagliola⁴ investigated the RZ chart to the condition assuming that each subgroup consists of $n > 1$ sample units. This extension is very important because, in several manufacturing environments, sample units can be changed due to planning decisions or cannot be ensured with sufficient precision. The statistic they suggest monitoring is

$$\hat{Z}_i = \frac{\sum_{j=1}^n X_{i,j}}{\sum_{j=1}^n Y_{i,j}}$$

Therefore the control limits are now

$$\begin{aligned} \text{UCL}_{RZ} &= F_{\hat{Z}_i}^{-1}\left(1 - \frac{\alpha}{2} \middle| n, \gamma_X, \gamma_Y, \omega_0, \rho_0\right) \\ \text{LCL}_{RZ} &= F_{\hat{Z}_i}^{-1}\left(\frac{\alpha}{2} \middle| n, \gamma_X, \gamma_Y, \omega_0, \rho_0\right) \end{aligned}$$

where

$$F_{\hat{Z}_i}^{-1}\left(p \middle| n, \gamma_X, \gamma_Y, \omega_0, \rho_0\right) = F_Z^{-1}\left(p \middle| n, \frac{\gamma_X}{\sqrt{n}}, \frac{\gamma_Y}{\sqrt{n}}, \frac{z_0 \gamma_X}{\gamma_Y}, \rho_0\right)$$

The fact that the size of each sample unit is not strictly fixed when considering different subgroups simplifies the quality control procedure and makes the chart implementation more flexible. Always the same example in the food industry, the quality practitioner decides to sample $n = 5$ boxes every 30 minutes, and they computed the ratio of the sample average weights of pumpkin seeds and flax seeds from the muesli mixture. The RZ-Shewhart chart immediately signals the occurrence of the out-of-control condition by plotting to point #12 above UCL_{RZ} .

2.2.2 Synthetic RZ-charts

It is well known that Shewhart-type control charts are rather inefficient in some sensitive situations, for example, detecting small or moderate changes in a process. One of the advanced approaches is the synthetic control chart. They are a combination of a traditional chart and a conforming run-length (CRL) chart. These charts have been considered to maintain simplicity, be easy to implement and interpret by practitioners, and outperform traditional Shewhart charts. Furthermore, it supports the quality management strategy of many practitioners, who prefer waiting until the occurrence of a second point beyond the control limits before looking for an assignable cause. To monitor the ratio of two normal variables, these charts were denoted by Syn-RZ. Celano and Castagliola⁷ designed and implemented the Zyn-RZ control charts. They also gave an example of the food industry to illustrate this model. Like the RZ-model, besides the control limits UCL_{RZ} and LCL_{RZ} , we consider the CRL sub-chart monitors the CRL, which is defined as the number of inspected samples between two consecutive nonconforming samples. Therefore, the Syn-RZ control charts signal if and only if the plotting statistic of the RZ-Shewhart sub-chart plots outside the control limits ($\hat{Z}_j \notin [\text{LCL}_{RZ}, \text{UCL}_{RZ}]$) and $\hat{Z}_k \in [\text{LCL}_{RZ}, \text{UCL}_{RZ}]$ for $k \in \{j + 1, j + 2, \dots, i - 1\}$ the resulting CRL is less than or equal to the H ($\text{CRL} = i - j \leq H$ with some $H \in \mathbb{N}^*$ defined by the practitioners). The statistical design of the Syn-RZ charts is an optimization problem

$$(H^*, \alpha_{RZ}^*) = \underset{(H, \alpha_{RZ})}{\text{argmin}} \text{ARL} \left[(H, \alpha_{RZ}) \middle| n, \gamma_X, \gamma_Y, \rho_0, \rho_1, \tau \right] \quad (5)$$

subject to

$$\text{ARL} \left[(H, \alpha_{RZ}) \middle| n, \gamma_X, \gamma_Y, \rho_0, \rho_1, \tau \right] = \text{ARL}_0$$

Here τ is the shift size. The numeric results allow us to conclude that the optimal value H^* increases for moderate to small shift size. The Syn-RZ charts improve its detection performance for the smaller coefficient of variation (γ_X, γ_Y). The authors also gave a table showing that the Syn-RZ charts significantly outperform the RZ charts in Celano and Castagliola⁴.

2.2.3 Runs Rules RZ charts

The statistical sensitivity of a Shewhart control chart can be improved by implementing supplementary Run Rules. Tran et al.⁸ adopted the run rules for the Shewhart-RZ control charts, denoted as RR-RZ control charts, to increase its sensitivity to small shifts. A Run Rules charts (denoted by $\text{RR}_{r,s}$) monitor the statistics X considering that the process is out-of-control, at instant i , if one of the following rules applies

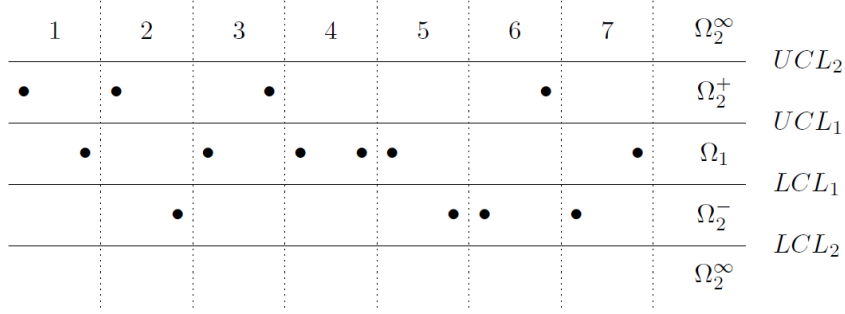


Figure 3: Intervals of $\Omega_1, \Omega_2^+, \Omega_2^-, \Omega_2^\infty$ and an example of transient states of the Markov chain $RR_{2,3} - X$

- $X_i \in \Omega_2^\infty$
- $X_i \in \Omega_2^-$ and $\#\{X_j \in \Omega_2^-, j = i - s + 1, \dots, i\} \geq r$ or $X_i \in \Omega_2^+$ and $\#\{X_j \in \Omega_2^+, j = i - s + 1, \dots, i\} \geq r$

where the domain of definition of Ω_2^+, Ω_2^- and Ω_2^∞ are in Fig 3

In order to compute the statistical properties of the RR-RZ control charts, they defined

- a lower-sided r -out-of- s Run Rules control chart (denoted as $RR-RZ_{r,s}^-$). An out-of-control signal is given at time i if $\hat{Z}_i < LCL_{RR-RZ}$ (in this case, $UCL_{RR-RZ} = +\infty$).
- an upper-sided r -out-of- s Run Rules control chart (denoted as $RR-RZ_{r,s}^+$). An out-of-control signal is given at time i if $\hat{Z}_i > UCL_{RR-RZ}$ (in this case, $LCL_{RR-RZ} = -\infty$).

A comparison with the ARL values for the RZ control chart was established. As expected, the RR-RZ charts are more sensitive than RZ charts to small shifts of the nominal ratio z_0 . Namely, it shows that in general, the shift-size $\tau \in [0.95, 1)$, the better option is $RR-RZ_{(r,s)}^-$ charts; when $\tau \in (1, 1.02]$, the better option is $RR-RZ_{(r,s)}^+$ chart and if $\tau < 0.95$ or $\tau > 1.02$, the better option is the RZ control chart (see Tran et al. ⁸).

2.2.4 EWMA RZ charts

One of the control chart types that we cannot ignore is the EWMA type. In these types of charts, instead of averages or individual observations, a smoothed moving average is applied to make any trend or deviation (in averages away from the center line) more apparent. These charts take full advantage of the previous sample information, making charts faster at detecting relatively small shifts. For example, Tran et al. ⁹ proposed two one-sided EWMA-RZ charts, and it turned out that the EWMA-RZ chart is statistically more sensitive than the Shewhart -RZ chart on the whole. The reason for choosing two one-sided instead of one two-sided was explained by the authors: in general, the ratio distribution can be asymmetrical, and designing two one-sided charts will be more flexible for practitioners. They looked at two sub-charts:

- an upward EWMA-RZ chart (denoted as $EWMA-RZ^+$) with a single control limit UCL^+ (here $LCL^+ = z_0$)

$$Y_i^+ = \begin{cases} \max(z_0, (1 - \lambda^+)Y_{i-1}^+ + \lambda^+\hat{Z}_i) & \text{if } i \geq 1 \\ z_0 & \text{if } i = 0 \end{cases}$$

- a downward EWMA-RZ chart (denoted as EWMA-RZ⁻) with a single control limit LCL⁻ (here UCL⁻ = z₀)

$$Y_i^- = \begin{cases} \min(z_0, (1 - \lambda^-)Y_{i-1}^- + \lambda^- \hat{Z}_i) & \text{if } i \geq 1 \\ z_0 & \text{if } i = 0 \end{cases}$$

here $\lambda^\pm \in (0, 1]$ is smooth parameter

The design of two one-sided EWMA-RZ charts consists in optimizing a couple λ and the control limit such that the value of out-of-control ARL is smallest.

If the ARL values for the out-of-control process are uniformly smaller than the in-control ARL, it is called an ARL-unbiased control chart. Otherwise, it takes a longer time on average to signal some assignable causes than when there is no assignable cause. In this case, control limits are chosen such that the ARL takes its maximum value at $\tau = 1$. Tran and Knoth¹⁰ studied the long-term properties of ARL-unbiased EWMA-RZ control chart, they also investigated the steady-state ARL. Their results show that when $\Delta_\tau = |\tau - 1|$ increase, the values optimal λ^* increase to 1; the performance of ARL-unbiased EWMA-RZ charts depends strongly on the sample size n and the value of (γ_X, γ_Y) . Their report indicates that the unbiased ARL limits exhibit the most balanced performance in both the zero-state and steady-state ARL. Hence, it is an attractive version of a two-sided EWMA RZ control chart.

2.2.5 CUSUM-RZ charts

In this type of chart, instead of plotting individual observations, a cumulative sum of the deviations of the individual measurements from the central line or target specifications is plotted. These charts are particularly powerful for detecting small shifts: While in traditional Shewhart charts, such a deviation does not generate an out-of-control condition within a large number of samples, the CUSUM chart is very sensitive in this respect and quickly detects such slight changes. Tran et al.¹¹ proposed and investigated the statistical properties of two Phase II one-sided CUSUM control charts for monitoring the ratio of population means of a bi-variate normal distribution $\hat{Z}_i = \sum_{j=1}^n X_{i,j} / \sum_{j=1}^n Y_{i,j}$. More specifically, they suggest the following two separate one-sided CUSUM charts:

- upward CUSUM-RZ with the corresponding upper control limit $ULC^+ = H^+ \times z_0$

$$S_i^+ = \begin{cases} \max(0, S_{i-1}^+ + \hat{Z}_i - z_0 + K^+) & \text{if } i \geq 1 \\ 0 & \text{if } i = 0 \end{cases}$$

- downward CUSUM-RZ with the corresponding lower control limit $LCL^- = H^- \times z_0$

$$S_i^- = \begin{cases} \max(0, S_{i-1}^- - (\hat{Z}_i - z_0) - K^-) & \text{if } i \geq 1 \\ 0 & \text{if } i = 0 \end{cases}$$

where z_0 is the in-control ratio and K^+, K^- are the reference parameters that tune the sensitivity of the corresponding CUSUM-RZ charts.

The aim of their work is to find out the optimal couples $(K^{\pm*}, H^{\pm*})$ by minimizing the out-of-control ARL according to the target in-control average run length (ARL₀). The numeric results show a similar tendency to the results in Celano and Castagliola⁴. As expected, compared to the Shewhart-RZ charts, the one-sided CUSUM-RZ control charts have significantly better performance in the detection of out-of-control conditions.

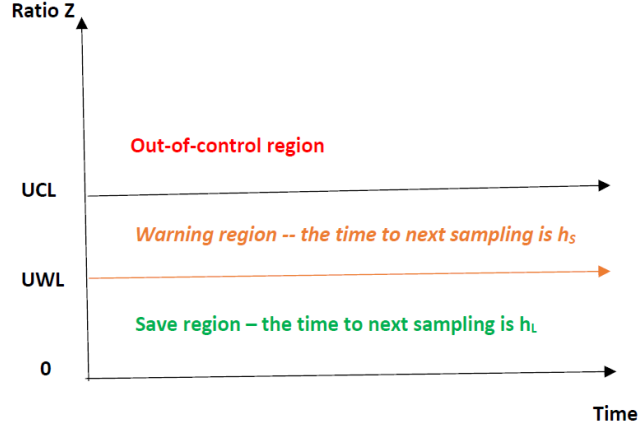


Figure 4: The upward VSI Shewhart-RZ chart

2.3 Adaptive control charts types of ratio

An adaptive control chart involves varying at least one of the chart’s parameters, such as the sampling interval, sample size, or the width constant of control limits. The purpose of this adaptive chart type is to improve the effectiveness of the control chart (i.e. detect out-of-control situations as quickly as possible). Varying the sampling interval (VSI) between samples is an alternative method adopted for quicker detection of an out-of-control process as compared with the conventional fixed sampling interval (FSI) Shewhart chart. The principle of this type is that the time until the next sample depends on what is being observed in the current sample. Sampling is less frequent when the process is at a high level of quality and vice versa. Nguyen et al.¹² suggest integrating the VSI feature into the Shewhart chart for monitoring the ratio of population means of a bivariate normal distribution. It is demonstrated that the FSI RZ charts are slower than VSI-type charts in detecting process changes. The domain of in-control is divided into two: one is the “save region” where the time to next sampling is h_L (“long”) and the “warning region” where the time to next sampling is h_S (“short”). Because of the property asymmetric of the distribution of the ratio, the run length (ARL) is biased. In order to overcome this drawback, the researcher proposes designing two separate one-sided control charts, involving an upper-sided chart, which detects an increase in the ratio (denoted as “upward Shewhart-RZ chart”), and a lower-sided chart, which detects a decrease in the ratio (denoted as “downward Shewhart-RZ chart”). For example, to illustrate the upper situation, we can look at Figure 4. Instead of looking at the ARL, they are looking for the average time to signal (ATS) which counts the expected time before a control chart signals an out-of-control condition after the occurrence of an assignable cause or the issue of a false alarm.

$$ATS = E(h) \times ARL \quad (6)$$

where $E(h) = (h_S p_S + h_L p_L) / (1 - q)$ is the average sampling interval. Here p_S, p_L , and q are the probabilities that a sample point drops into the safe, warning, and out-of-control regions, respectively.

For the type EWMA and CUSUM, the readers can refer to Nguyen et al.¹³ and Nguyen et al.¹⁴.

2.4 RZ - control charts under the effect of measurement errors

To enhance the practical use of the ratio chart, the effect of measurement error has been considered in recent times. Most studies show that both the precision error and the accuracy error have negative

impacts on the performance of the control chart. In this model, under the presence of measurement error, the observations at time i will be

$$\mathbf{W}_{i,j,k}^* = \mathbf{A} + \mathbf{B}\mathbf{W}_{i,j} + \varepsilon_{i,j,k}, k = 1, \dots, m, \quad (7)$$

where $\mathbf{W}_{i,j} = (X_{i,j}, Y_{i,j})^T \sim N(\boldsymbol{\mu}_{\mathbf{W}}, \boldsymbol{\Sigma}_{\mathbf{W}})$ is a bi-variate normal vector with mean $\boldsymbol{\mu}_{\mathbf{W}}$ and variance-covariance matrix $\boldsymbol{\Sigma}_{\mathbf{W}}$, $\mathbf{A} = (a_X, a_Y)^T$ is a (2×1) constants vector, \mathbf{B} is a (2×2) matrix, $\varepsilon \sim N(\mathbf{0}, \boldsymbol{\Sigma}_M)$ is a centered bivariate normal random vector assumed to be independent of \mathbf{W} .

The monitoring statistics

$$\hat{Z}_i^* = \frac{\hat{\mu}_{X_i^*}}{\hat{\mu}_{Y_i^*}} = \frac{\sum_{j=1}^n \bar{X}_{i,j}^*}{\sum_{j=1}^n \bar{Y}_{i,j}^*}, \quad (8)$$

are recommended, where $\bar{X}_{i,j}^*$ and $\bar{Y}_{i,j}^*$ are two components of the bi-variate normal vector $\bar{\mathbf{W}}_{i,j}^*$.

In literature, we found that some models of RZ charts are considered with the effect of measurement errors like Shewhart-RZ charts (see Tran et al.¹⁵; Nguyen and Tran¹⁶), EWMA-RZ charts (see Nguyen et al.¹⁷), Run sum RZ charts (see Abubakar et al.¹⁸). Future research could be to investigate the effect of measurement errors on the control charts, monitoring the ratio of random normal variables like the CUSUM-RZ charts, Adaptive EWMA-RZ charts, Adaptive CUSUM-RZ charts, considering the case of short runs or considering Phase I implementation.

3 Monitoring the Compositional Data

CoDa and the ratio of two normal random variables are two types of data that deal with ratios or proportions of different components or variables. CoDa represents proportions or percentages of different components that sum up to a constant, while the ratio of two normal random variables represents the ratio of two continuous variables having normal distributions. Although these data types are distinct, they share a common aspect of involving relative information of two or more components or variables. The ratio of two normal variables can be regarded as a special case of CoDa in which the number of components is limited to two, and the data has a normal distribution in a Simplex space. Control charts can be used to monitor the ratios involved in both data types and detect process changes over time. Due to their shared feature of involving ratios or proportions, we decided to group the control charts for monitoring CoDa and the ratio of two normal variables together in our analysis and review.

3.1 Modelling of Compositional Data

This section presents a brief overview of the CoDa and its simplex space, as well as several widely-used transformation techniques to transform CoDa into a vector representation in real space.

In statistics, CoDa refers to data that often describes the proportions, percentages, concentrations, or frequencies of some whole, and their individual values are strictly positive. An example of CoDa is the mineral composition in a rock sample, where a geologist can obtain a rock sample and perform an analysis to determine the proportions of its various mineral components. The applications of CoDa can be found in many domains, including but not limited to chemical research, econometric and survey data analyses, geology, the food industry, etc. where the composition of a sample is important for understanding the properties or behavior of the system, see Aitchison².

According to the definition provided by Aitchison², Pawlowsky-Glahn et al.¹⁹, a (row) vector $\mathbf{x} = (x_1, \dots, x_p)$ is considered a p-part composition if its components are strictly positive and carry only relative information. The term “relative information” here refers to the interrelationships among the composition’s components, regardless of their numerical values. The sum of all the components of \mathbf{x} , $\sum_{i=1}^p x_i$, is a constant κ . Depending on the value of κ , the measurements can be interpreted as proportions (if $\kappa = 1$) or percentages (if $\kappa = 100$), for instance. Since the multiplication of a positive vector by a positive constant does not change the ratios between its components, each composition can be regarded as an equivalent class of proportional factors. Thus, if $\mathbf{x} = \lambda \mathbf{y}$ where \mathbf{x} and \mathbf{y} are compositions, and λ is a constant, we say that \mathbf{x} and \mathbf{y} are compositionally equivalent. Alternatively, the closure of a p-part composition $\mathbf{x} = (x_1, x_2, \dots, x_p)$ to $\kappa > 0$ is defined by

$$\mathcal{C}(\mathbf{x}) = \left(\frac{\kappa x_1}{\sum_{i=1}^p x_i}, \frac{\kappa x_2}{\sum_{i=1}^p x_i}, \dots, \frac{\kappa x_p}{\sum_{i=1}^p x_i} \right) \quad (9)$$

then the two p-part compositions are considered to be compositionally equivalent if their closures are equal, i.e., $\mathcal{C}(\mathbf{x}) = \mathcal{C}(\mathbf{y})$, for every positive constant κ .

The sample space of CoDa is represented by the simplex,

$$\mathcal{S}^p = \left\{ \mathbf{x} = (x_1, x_2, \dots, x_p) \mid x_i > 0, i = 1, \dots, p; \sum_{i=1}^p x_i = \kappa \right\} \quad (10)$$

In Euclidean space, vectors can be added or multiplied by scalars using Euclidean geometry to determine their properties or compute the distance between them. However, applying this geometry directly to CoDa in \mathcal{S}^p is not feasible due to its special structure. To address this issue, Aitchison introduced the Aitchison geometry, with two fundamental operations required for a vector space structure of the simplex \mathcal{S}^p : perturbation and powering operators. These operators are equivalent to the addition and multiplication by scalar operations in real space, respectively. The perturbation operation, denoted by \oplus , adds a vector $\mathbf{y} \in \mathcal{S}^p$ to a vector $\mathbf{x} \in \mathcal{S}^p$, and is defined as follows:

$$\mathbf{x} \oplus \mathbf{y} = \mathcal{C}(x_1 y_1, \dots, x_p y_p) \in \mathcal{S}^p$$

The powering operation, denoted by \odot , multiplies a vector $\mathbf{x} \in \mathcal{S}^p$ by a scalar constant $\alpha \in \mathbb{R}$, and is defined as follows

$$\alpha \odot \mathbf{x} = \mathcal{C}(x_1^\alpha, \dots, x_p^\alpha) \in \mathcal{S}^p$$

The simplex \mathcal{S}^p with the perturbation and the power operations result in a vector space structure, denoted by $(\mathcal{S}^p, \oplus, \odot)$.

In practical applications, it is common to transform CoDa into vectors in the Euclidean space rather than directly deploying the model in the Simplex space to eliminate the constraints of CoDa. One widely used transformation technique is the centered log-ratio transformation (clr) proposed by Aitchison². This clr transformation is an isometry from the Simplex space \mathcal{S}^p to a subspace $U \subset \mathbb{R}^p$, defined as follows

$$\text{clr}(\mathbf{x}) = \left(\ln \frac{x_1}{g_m(\mathbf{x})}, \ln \frac{x_2}{g_m(\mathbf{x})}, \dots, \ln \frac{x_p}{g_m(\mathbf{x})} \right) = (\xi_1, \xi_2, \dots, \xi_p) \quad (11)$$

Here, $g_m(\mathbf{x}) = \left(\prod_{i=1}^p x_i \right)^{\frac{1}{p}} = \exp \left(\frac{1}{p} \sum_{i=1}^p \ln x_i \right)$ represents the component-wise geometric mean of the

composition, and $\sum_{i=1}^p \xi_i = 0$. The inverse of the clr transformation retrieves \mathbf{x} from $\boldsymbol{\xi} = (\xi_1, \dots, \xi_p)$ by

$$\text{clr}^{-1}(\boldsymbol{\xi}) = \mathcal{C}(\exp(\boldsymbol{\xi})) = \mathcal{C}(\exp(\xi_1), \exp(\xi_2), \dots, \exp(\xi_p)). \quad (12)$$

According to Egozcue et al.²⁰, the constraint in the component of $\text{clr}(\mathbf{x})$ results in a singular variance-covariance matrix for random composition. To address this issue, Egozcue et al.²⁰ introduced a new transformation called the isometric log-ratio (ilr) transformation, which is associated with an orthogonal basis in \mathcal{S}^p . Let $\mathbf{e}_1, \mathbf{e}_2, \dots, \mathbf{e}_{p-1}$ be an orthonormal basis of \mathcal{S}^p , hence any composition $\mathbf{x} \in \mathcal{S}^p$ can be expressed as a linear combination of this basis, i.e.,

$$\mathbf{x} = \bigoplus_{i=1}^{p-1} x_i^* \odot \mathbf{e}_i, \quad x_i^* = \langle \text{clr}(\mathbf{x}), \text{clr}(\mathbf{e}_i) \rangle$$

The ilr transformation of $\mathbf{x} \in \mathcal{S}^p$ is given by $\text{ilr}(\mathbf{x}) = \mathbf{x}^* = (x_1^*, x_2^*, \dots, x_{p-1}^*)$.

Let \mathbf{B} be a $(p-1, p)$ matrix with the i^{th} row defined as $\text{clr}(\mathbf{e}_i)$, for $i = 1, \dots, p-1$. This matrix is commonly known as a contrast matrix associating to the orthonormal basis $\mathbf{e}_1, \mathbf{e}_2, \dots, \mathbf{e}_{p-1}$. The ilr transformation of a composition \mathbf{x} can be computed as follows:

$$\mathbf{x}^* = \text{ilr}(\mathbf{x}) = \text{clr}(\mathbf{x}) \cdot \mathbf{B}^\top$$

There are many orthonormal basis candidates for \mathcal{S}^p . One such candidate was proposed by Egozcue and Pawlowsky-Glahn²¹ using a sequential binary partition method. In this particular basis, \mathbf{e}_i is defined as $\mathcal{C}(e_{i,1}, \dots, e_{i,j}, \dots, e_{i,p})$, where

$$e_{i,j} = \begin{cases} \exp\left(\sqrt{\frac{1}{i(i+1)}}\right) & \text{if } j \leq i \\ \exp\left(-\sqrt{\frac{i}{i+1}}\right) & \text{if } j = i+1 \\ 1 & \text{otherwise} \end{cases}$$

Using this orthonormal basis to transform \mathbf{x} , the resulting coordinates x_i^* can be computed as

$$x_i^* = \sqrt{\frac{i}{i+1}} \ln \left(\frac{\left(\prod_{j=1}^i x_j\right)^{\frac{1}{i}}}{x_{i+1}} \right).$$

Given the ilr coordinate \mathbf{x}^* , the original composition \mathbf{x} can be recovered by applying the inverse ilr transformation as follows

$$\text{ilr}^{-1}(\mathbf{x}^*) = \text{clr}^{-1}(\mathbf{x}^* \mathbf{B}) = \mathcal{C}(\exp(\mathbf{x}^* \mathbf{B})).$$

Table 3 illustrates the practical application of the ilr transformation for the case where the number of parts p is 4. The first five columns of the table present the components of ten compositions in \mathcal{S}^5 , while the remaining three columns show their corresponding ilr coordinates in \mathbb{R}^4 . It can be observed that the ilr coordinates x_i^* are no longer constrained by the constant sum. For a more comprehensive understanding of CoDa and its properties, see Pawlowsky-Glahn et al.¹⁹.

x_1	x_2	x_3	x_4	x_5	x_1^*	x_2^*	x_3^*	x_4^*
0.02	0.3	0.14	0.25	0.29	-1.91	-0.48	-0.84	-0.82
0.15	0.08	0.22	0.3	0.25	0.44	-0.57	-0.67	-0.32
0.11	0.17	0.23	0.11	0.38	-0.31	-0.42	0.34	-0.82
0.01	0.08	0.22	0.08	0.61	-1.47	-1.67	-0.31	-2.04
0.39	0.1	0.33	0.07	0.11	0.96	-0.42	1.05	0.33
0.23	0.08	0.42	0.05	0.22	0.75	-0.92	1.19	-0.4
0.31	0.03	0.46	0.04	0.16	1.65	-1.28	1.21	-0.35
0.04	0.06	0.33	0.2	0.37	-0.29	-1.56	-0.67	-1.07
0.22	0.35	0.13	0.26	0.04	-0.33	0.62	-0.16	1.55
0.24	0.38	0.11	0.25	0.02	-0.32	0.82	-0.13	2.78

Table 3: Example of ilr transformation in \mathcal{S}^5

3.2 Control charts for monitoring CoDa

The first control chart for monitoring this special data was proposed by Boyles²², in which the author explored the application of a chi-square control chart for monitoring data (CoDa) derived from the Dirichlet distribution. The degrees of freedom in the chi-square distribution were adjusted slightly to accommodate this approach. Subsequently, other types of control charts, such as Shewhart-type and memory-type charts, were also developed and examined. These control charts adhere to the same principles as conventional control charts but have been adapted to accommodate the special structure of CoDa, including its non-negative components and constant-sum constraints. The log-ratio transformation method is commonly employed in this context, as mentioned in Section 3. In this section, a brief review of research related to control charts for monitoring CoDa in Phase II MSPC will be provided.

3.2.1 Chi-square control chart

The chi-square control chart was initially proposed by Boyles²² when studying CoDa derived from a Dirichlet distribution. Given a sample of size n independent observations $\mathbf{x}_1, \mathbf{x}_2, \dots, \mathbf{x}_n$ where $\mathbf{x}_i = (x_{i1}, x_{i2}, \dots, x_{ip})$ follows a Dirichlet distribution $\mathcal{D}(\alpha)$ with $\alpha = (\alpha_1, \alpha_2, \dots, \alpha_p)$ is a positive parameter, the statistic of interest to be monitored is given by

$$X^2 = \frac{(x_{i1} - \pi_1)^2}{\pi_1} + \frac{(x_{i2} - \pi_2)^2}{\pi_2} + \dots + \frac{(x_{ip} - \pi_p)^2}{\pi_p}, \quad (13)$$

where $\pi_1, \pi_2, \dots, \pi_p$ denote the process averages. Boyles²² demonstrated that when the CoDa originate from a Dirichlet distribution, X^2 is asymptotically distributed as a multiple of χ_{p-1}^2 , thereby the X^2

chart based on χ_{p-1}^2 valid as a certain type of asymptotic approximation. To achieve an overall false alarm rate of 0.0027, the upper control limit has been established based on the “ 3σ ” threshold.

3.2.2 Shewhart-type control charts

Guevara et al.²³ pioneered the application of Hotelling T^2 control charts in Dirichlet regression to examine the connection between a response variable and one or more explanatory variables. Subsequently, Vives-Mestres et al.²⁴ studied a method for interpreting out-of-control signals in the T_C^2 control chart used for monitoring three-part CoDa. Building upon this work, Vives-Mestres et al.²⁵ proposed an extension of the T_C^2 chart to monitor individual CoDa observations based on isometric log-ratio (ilr) transformation. In these works, the authors conducted an investigation on the control charts to detect shifts in the mean vector and assumed that the covariance matrix of the distribution would remain constant throughout the study. Furthermore, they presumed that the in-control (IC) and out-of-control (OC) distributions of the dataset followed a normal distribution. The general design of the T_C^2 chart is as follows: Let $\mathbf{x}_1, \mathbf{x}_2, \dots$, be Phase II p-parts compositions with the in-control (IC) data follows a normal distribution $\mathcal{N}(\boldsymbol{\mu}_0, \boldsymbol{\Sigma}_0)$ on the simplex space \mathcal{S}^p . Let $\mathbf{x}_i^* = (x_{i1}^*, x_{i2}^*, \dots, x_{i,p-1}^*)$ denote its ilr coordinates (as defined in Section 3) then \mathbf{x}_i^* follows a normal distribution $\mathcal{N}(\boldsymbol{\mu}_0^*, \boldsymbol{\Sigma}_0^*)$ in the real space \mathbf{R}^{p-1} . In case $\boldsymbol{\mu}_0^*, \boldsymbol{\Sigma}_0^*$ are known, the monitored statistic of this T_C^2 at i^{th} time point is defined by

$$T_C^2 = (\mathbf{x}_i^* - \boldsymbol{\mu}_0^*)' \boldsymbol{\Sigma}_0^{*-1} (\mathbf{x}_i^* - \boldsymbol{\mu}_0^*) \quad (14)$$

and the chart would give a signal of mean shift if $T_C^2 > \chi_{1-\alpha, p-1}^2$ where $\alpha \in [0, 1]$ is the given significant level, $\chi_{1-\alpha, p-1}^2$ is the $100(1 - \alpha)$ -th quantile of χ_{p-1}^2 distribution. In scenarios where both $\boldsymbol{\mu}_0^*$ and $\boldsymbol{\Sigma}_0^*$ are unknown, as is frequently encountered in practical applications, they can be estimated using the sample mean vector $\bar{\mathbf{x}}$ and the sample covariance matrix \mathbf{S} of the ilr transformed data of the IC sample (obtain from Phase I). Suppose that an IC sample of size n is available, the T_C^2 statistic at i^{th} time point becomes

$$T_C^2 = (\mathbf{x}_i^* - \bar{\mathbf{x}})' \mathbf{S}^{-1} (\mathbf{x}_i^* - \bar{\mathbf{x}}) \quad (15)$$

and the chart would give a signal of mean shift when $T_C^2 > \frac{(p-1)(n-1)(n+1)}{n(n-p-1)} \mathcal{F}_{1-\alpha, p-1, n-p-1}$ where $\mathcal{F}_{1-\alpha, p-1, n-p-1}$ is the $100(1 - \alpha)$ -th quantile of \mathcal{F} distribution $\mathcal{F}_{p-1, n-p-1}$.

Vives-Mestres et al.²⁵ compared this T_C^2 chart using ilr transformation method to transform CoDa with the T^2 control chart after removing one component of the composition and has shown its out-performance with the other in terms of average run length (ARL) values. However, it (and Hotelling’s T^2 control chart for monitoring other types of data) has a significant drawback in that it assumes that the variance-covariance matrix of the process is constant over time, which may not always hold in practical situations. Changes in raw materials, process parameters, equipment, environmental conditions, personnel, and other factors can lead to variability in the covariance matrix of the process, making the chart less effective in detecting changes in the process over time. Additionally, the control chart makes decisions about process performance solely based on the observed data at the current time point, which can be less sensitive to small shifts in the process distribution. This can lead to a higher probability of false alarms and missed opportunities to identify and correct process issues.

3.2.3 Memory-type control charts

As in unconstrained cases and as mentioned before, multivariate Shewhart charts used for monitoring CoDa assume that the variance-covariance matrix of the process is constant over time and relies only on the observed data at the current time point to make decisions about process performance.

While they effectively detect relatively large and transient shifts, they are less sensitive to relatively small and persistent shifts in the process distribution. To address these limitations, researchers have suggested using multivariate control charts such as multivariate exponentially weighted moving average (MEWMA) and multivariate cumulative sum (MCUSUM), which incorporate the information from previous observations along with the current observation, improving their ability to detect small shifts. These memory-type control charts use both past and present observations to make decisions and update their estimates over time.

Suppose that at each sampling period $i = 1, 2, \dots$, a sample of size m independent p -part compositions $\mathbf{x}_{i,1}, \dots, \mathbf{x}_{i,m}$ is collected and each $\mathbf{x}_{i,j}$ follows a multivariate normal distribution $N_{\mathcal{S}^p}(\boldsymbol{\mu}, \boldsymbol{\Sigma})$, on the simplex \mathcal{S}^p . Assume also that when the process is in control, the composition center is $\boldsymbol{\mu}_0$, and when the process is out-of-control, the composition center is $\boldsymbol{\mu}_1$. Let $\mathbf{x}_{i,1}^*, \dots, \mathbf{x}_{i,m}^*$ represent the ilr coordinates of $\mathbf{x}_{i,1}, \dots, \mathbf{x}_{i,m}$ hence $\mathbf{x}_{i,j}^*$ follows a multivariate normal distribution, $\mathcal{N}_{\mathbb{R}^{p-1}}(\boldsymbol{\mu}_0^*, \boldsymbol{\Sigma}_0^*)$, on \mathbb{R}^{p-1} .

- **Multivariate EWMA-CoDa control charts**

Tran et al.²⁶ proposed to use a MEWMA scheme to monitor CoDa. The statistic to monitor the process suggested by Tran et al.²⁶ is

$$Q_i = \mathbf{w}_i^\top \boldsymbol{\Sigma}_{\mathbf{w}_i}^{-1} \mathbf{w}_i, i = 1, 2, \dots \quad (16)$$

where

$$\mathbf{w}_i = r(\bar{\mathbf{x}}_i^* - \boldsymbol{\mu}_0^*) + (1 - r)\mathbf{w}_{i-1}, i = 1, 2, \dots \quad (17)$$

is the EWMA vector, $\bar{\mathbf{x}}_i^*$ is the sample mean of i^{th} ilr-transformed sample, $\boldsymbol{\Sigma}_{\mathbf{w}_i}$ is the variance-covariance matrix of \mathbf{w}_i . The smoothing parameter r in the EWMA vector determines the weights given to the current and past observations. A higher value of r results in a faster decrease in the weights given to past observations, meaning that past observations have less influence on the MEWMA statistic and vice versa. The MEWMA chart issues an out-of-control signal when the value of the statistic Q_i exceeds the upper control limit H , where H is chosen to achieve a specific in-control average run length (ARL_0).

- **Multivariate CUSUM-CoDa control chart**

Imran et al.²⁷ considered the MCUSUM-CoDa control chart in both known and unknown parameters cases. In case $\boldsymbol{\mu}_0^*, \boldsymbol{\Sigma}_0^*$ are known, the monitoring statistic of the MCUSUM-CoDa will be

$$C_i = [m(\mathbf{s}_i^T \boldsymbol{\Sigma}_0^{*-1} \mathbf{s}_{i-1})]^{1/2}, i = 1, 2, \dots \quad (18)$$

where

$$\mathbf{s}_i = \begin{cases} 0 & \text{if } i = 0 \text{ or } Q_i \leq k \\ (\mathbf{s}_{i-1} + \bar{\mathbf{x}}_i^* - \boldsymbol{\mu}_0^*)(1 - k/Q_i) & \text{otherwise} \end{cases}$$

$$Q_i = \left(m(\mathbf{s}_{i-1} + \bar{\mathbf{x}}_i^* - \boldsymbol{\mu}_0^*)^T \boldsymbol{\Sigma}_0^{*-1} (\mathbf{s}_{i-1} + \bar{\mathbf{x}}_i^* - \boldsymbol{\mu}_0^*) \right)^{1/2}$$

This MCUSUM-CoDa chart issues a signal when $C_i > h$, where h is chosen to achieve a specific value of in-control ARL. In case $\boldsymbol{\mu}_0^*, \boldsymbol{\Sigma}_0^*$ are unknown, they can be estimated by the sample mean

and sample covariance matrix of the available IC dataset

$$\hat{\boldsymbol{\mu}}_0^* = \frac{1}{n} \sum_{j=1}^n \bar{\mathbf{x}}_j^*, \quad \hat{\boldsymbol{\Sigma}}_0^* = \frac{1}{n} \sum_{j=1}^n \mathbf{S}_j^* \quad (19)$$

where n is the number of samples of size m IC data, \mathbf{S}_j^* is the sample covariance matrix of j^{th} sample. The MCUSUM-CoDa chart has been demonstrated to exhibit similar performance to the MEWMA-CoDa chart and to outperform the T^2 -CoDa chart in terms of ARL values.

3.2.4 Adaptive control charts

- **VSI MEWMA-CoDa control chart:**

As an extension of the MEWMA-CoDa chart, Nguyen et al.²⁸ designed a Phase II MEWMA-CoDa control chart with variable sampling intervals to monitor CoDa based on isometric log-ratio transformation. In the FSI MEWMA-CoDa control chart, the sampling interval is set at a consistent value denoted as h_F . Conversely, in the VSI MEWMA-CoDa control chart, the interval between consecutive samples $\bar{\mathbf{X}}_i, \bar{\mathbf{X}}_{i+1}$ changes based on the present value of Q_i . This chart maintains the same UCL as the FSI chart but adds an extra warning limit, represented as $w = \text{UWL}$ where $0 < \text{UWL} < \text{UCL}$. This warning limit helps switch between longer (h_L) and shorter (h_S) sampling intervals. The longer interval h_L is used when the control statistic $Q_i^2 \leq \text{UWL}^2$ indicates a safe zone, and the shorter interval h_S is applied when $\text{UWL}^2 < Q_i^2 \leq \text{UCL}^2$, marking a warning zone. A signal indicating the process is out of control is generated when $Q_i^2 > \text{UCL}^2$. As the sampling interval in the VSI chart is variable, the relationship between Average Time to Signal (ATS) and Average Run Length (ARL) in this chart can be expressed as:

$$\text{ATS}^{\text{VSI}} = E(h) \times \text{ARL}^{\text{VSI}} \quad (20)$$

Here, $E(h)$ signifies the average sampling interval. The proposed FSI MEWMA-CoDa control chart has shown its better performance compared with the original version of MEWMA-CoDa in terms of Average Time to Signal (ATS) values.

- **VSS MEWMA-CoDa control chart:**

Traditionally, standard process monitoring control charts have primarily relied on a fixed sample size (FSS) approach. As another extension to the MEWMA-CoDa chart,²⁹ proposed a control chart that leverages a variable sample size (VSS), namely VSS-MEWMA-CoDa, to enhance the efficiency and effectiveness of the MEWMA control chart when applied to CoDa. In this work, the MEWMA vectors are calculated by

$$\mathbf{w}_i = r\hat{\mathbf{z}}_i + (1 - r)\mathbf{w}_{i-1}, \quad (21)$$

where $\hat{\mathbf{z}}_i$ is the standardized sample mean of i^{th} ilr-transformed sample with

$$\hat{\mathbf{z}}_i = \frac{\hat{\mathbf{x}}_i^* - \boldsymbol{\mu}_0^*}{\sigma_0^*/\sqrt{n}}.$$

The asymptotic variance-covariance matrix proposed by Lowry et al.³⁰ is commonly used to estimate the variance-covariance matrix $\boldsymbol{\Sigma}_{W_i}$

$$\boldsymbol{\Sigma}_{W_i} = \frac{r}{n(2 - r)} \boldsymbol{\Sigma}^* \quad (22)$$

The VSS-MEWMA-CoDa CC issues a signal when the statistic Q_i with

$$Q_i = \mathbf{w}_i^\top \boldsymbol{\Sigma}_{\mathbf{w}_i}^{-1} \mathbf{w}_i, i = 1, 2, \dots \quad (23)$$

is greater than the upper control limit (UCL). The sample size n is varied based on the value of statistic Q_i . The transition from a small to a large sample size, or vice versa, is based on the computed value of Q_i . Specifically, a smaller sample size is employed, denoted as $n = n_1$, when the value of Q_i falls within the range $0 < Q_i < \text{UWL}$. Conversely, a larger sample size, indicated by $n = n_2$, is utilized when Q_i satisfies the condition $\text{UWL} < Q_i < \text{UCL}$. It is important to note that n_1 , n_0 , and n_2 are related such that $n_1 < n_0 < n_2$, where n_0 represents the predetermined fixed sample size.

3.2.5 Control charts under the effect of measurement error or autocorrelation between samples

- **Control charts under the effect of measurement error**

The impact of measurement error on control chart performance has been a focal point of research in statistical process monitoring, drawing attention to the need for addressing such errors to maintain the integrity of control charts, particularly those dealing with CoDa. The groundwork in this area was set by Zaidi et al.³¹, who investigated the effect of measurement errors on the performance of the Hotelling T^2 control chart for CoDa. In this work, the authors defined the sample mean composition at time i by

$$\bar{\mathbf{x}}_i = \frac{1}{m}(\mathbf{x}_{i1} \oplus \dots \oplus \mathbf{x}_{im}) = \mathbf{a} \oplus (b \cdot \mathbf{y}_i) \oplus \frac{1}{m}(\epsilon_{i1} \oplus \dots \oplus \epsilon_{im}).$$

where $\mathbf{a} \in \mathcal{S}^p$ and $b \in \mathbb{R}$ are known constants, ϵ_{ij} is a multivariate normal random error term $\text{MNOR}_{\mathcal{S}^p}(\mathbf{0}, \boldsymbol{\Sigma}_M^*)$ that accounts for measurement inaccuracies, and $\boldsymbol{\Sigma}_M^*$ is the known measurement error variance-covariance matrix. The Hotelling T^2 control chart accounts for measurement errors through the statistic:

$$Z_i = (\bar{\mathbf{x}}_i^* - \mathbf{a}^* - b\boldsymbol{\mu}_0^*) \left(b^2 \boldsymbol{\Sigma}^* + \frac{1}{m} \boldsymbol{\Sigma}_M^* \right)^{-1} (\bar{\mathbf{x}}_i^* - \mathbf{a}^* - b\boldsymbol{\mu}_0^*)^T.$$

Building upon this, Zaidi et al.³² furthered the discourse by incorporating measurement errors into the MEWMA-CoDa control chart analysis, which provided insights into the implications for production processes. In a continued effort to unravel the effect of measurement errors, Imran et al.³³ examined their influence on the multivariate CUSUM control charts. Most recently, Imran et al.³⁴ emphasized the critical role of measurement error in the VSI Hotelling T^2 charting scheme. These studies highlight the evolving recognition of measurement error as a significant factor that affects the efficacy of control charts in ensuring quality and reliability in manufacturing processes.

- **CoDa control chart for autocorrelated data**

In the SPC, it is a standard presumption that data is independent and lacks autocorrelation. However, this assumption does not hold true in many practical industrial applications, especially when dealing with CoDa. This prevalent autocorrelation within CoDa vectors poses a challenge, as it can significantly impair the interpretative accuracy of control chart signals and diminish their capacity for detecting anomalies. Addressing this issue, Zaidi et al.³⁵ introduced the application of a time series autoregressive moving average (ARMA) model to manage autocorrelated CoDa within the simplex space \mathcal{S}^p . The ARMA model for CoDa is written as:

$$\mathbf{x}_t = \alpha_1 \otimes \mathbf{x}_{t-1} \oplus \cdots \oplus \alpha_p \otimes \mathbf{x}_{t-p} \oplus \boldsymbol{\epsilon}_t \ominus \beta_1 \otimes \boldsymbol{\epsilon}_{t-1} \oplus \cdots \oplus \beta_q \otimes \boldsymbol{\epsilon}_{t-q},$$

where $\boldsymbol{\alpha} = (\alpha_1, \dots, \alpha_p)$ and $\boldsymbol{\beta} = (\beta_1, \dots, \beta_q)$ are the unknown parameters, p, q are the order of autoregressive polynomial and moving average polynomial, respectively, and $\boldsymbol{\epsilon}_t$ is the residual term. The residual control chart for CoDa is applied by assuming a multivariate normal distribution within the simplex space. Specifically, where the residual vector $\boldsymbol{\epsilon}$ follows a multivariate normal distribution $\text{MNOR}_{\mathcal{S}^p}(\boldsymbol{\mu}_\epsilon, \boldsymbol{\Sigma}_\epsilon)$ in the simplex space \mathcal{S}^p , the Hotelling T^2 control chart for residuals is formulated as:

$$T^2 = (\boldsymbol{\epsilon}^* - \bar{\boldsymbol{\epsilon}}^*)(\boldsymbol{\Sigma}_\epsilon^*)^{-1}(\boldsymbol{\epsilon}^* - \bar{\boldsymbol{\epsilon}}^*)^T,$$

where $\boldsymbol{\epsilon}^*$ is the ilr-transformed residual vector, $\bar{\boldsymbol{\epsilon}}^*$ is the estimator of the mean vector $\boldsymbol{\mu}_\epsilon$, and $\boldsymbol{\Sigma}_\epsilon^*$ is the estimator of variance-covariance matrix $\boldsymbol{\Sigma}_\epsilon$. The Hotelling T^2 control chart that utilizes residuals from the CoDa ARMA model demonstrated superior performance in detecting shifts in the mean vector when compared to the Hotelling T^2 based on isometric log-ratio transformed original data. This enhancement underscores the critical importance of accounting for autocorrelation in SPC to ensure the reliability of quality monitoring techniques.

3.3 Analysis

In this section, we present a comprehensive analysis of the papers collected for reviewing the topic of monitoring CoDa. Through a series of visualizations and summary tables, we aim to provide a clear and insightful overview of the research landscape in this field. The analysis includes the distribution of papers across various research categories, the publication trends over time, and a detailed breakdown of the journals that have featured this research, as well as the key contributions of leading authors in this field.

Table 4 provides a quick reference to key aspects across the 19 collected papers on monitoring CoDa, spanning from 1997 to 2023. It delineates the progression and scope of research through various facets such as control chart categorizations, the number of p-parts of the CoDa vector, the transformation/analyzing method, and comparison between the proposed control chart (if available).

In order to provide a clear overview of the research focus in the field of monitoring CoDa, Fig. 5 provides a pie chart category of 19 papers in distinct research categories: Shewhart type, Memory type, Adaptive type, Control charts for monitoring CoDa under the influence of Measurement Error and Autocorrelation, and Others type. This visual representation highlights the proportions of research efforts dedicated to each category, offering insights into the most heavily researched areas and those that may require further exploration. According to the pie chart, Shewhart-type control charts, a classic in the field, account for 26% of the papers, indicating their importance in monitoring CoDa. Similarly, control charts considering the measurement error and autocorrelation also make up 26%, highlighting the importance of considering the effect of measurement error and the intricacies of data dependencies in monitoring. Adaptive control charts represent 21%, reflecting their popularity of consideration in this field. Notably, 11% of the papers integrate artificial intelligence with control charts, pointing towards an innovative direction that could redefine future methodologies.

Papers	Control chart	Type	N^0 of p-part	Transformation /Analyzed method	Comparison with other charts	Best chart
Boyles ²²	Chi-square	Shewhart-type	Arbitrary	No transformation	-	-
Guevara et al. ²³	T^2	Shewhart-type	Arbitrary	Dirichlet Regression	-	-
Vives-Mestres et al. ²⁴	T^2	Shewhart-type	p = 3	ilr	-	-
Vives-Mestres et al. ²⁵	T^2	Shewhart-type	p = 3	ilr	-	-
Vives-Mestres et al. ³⁶	T^2	Shewhart-type	Arbitrary	clr	-	-
Tran et al. ²⁶	MEWMA	Memory-type	Arbitrary	ilr	T^2	MEWMA
Zaidi et al. ³¹	T^2	ME/Autocorrelation	Arbitrary	ilr	-	-
Zaidi et al. ³²	MEWMA	ME/Autocorrelation	Arbitrary	ilr	T2	MEWMA
Nguyen et al. ²⁸	VSI-MEWMA	Addaptive	Arbitrary	ilr	MEWMA	VSI-MEWMA
Imran et al. ²⁷	MCUSUM	Memory-type	Arbitrary	ilr	T2, MEWMA	CUSUM, MEWMA
Imran et al. ³³	CUSUM	ME/Autocorrelation	Arbitrary	ilr	-	-
Imran et al. ²⁹	VSS-MEWMA	Addaptive	Arbitrary	ilr	FSS-MEWMA	VSS-MEWMA
Imran et al. ³⁷	VSI-MEWMA	Addaptive	Arbitrary	ilr	FSI-MEWMA	VSI-MEWMA
Weiß ³⁸	Ordinal	Others	Arbitrary	alr	-	-
Zaidi et al. ³⁵	T^2_{ARMA}	ME/Autocorrelation	Arbitrary	T^2 , CoDa ARMA	T^2	T^2_{ARMA}
Imran et al. ³⁴	VSI T^2	ME/Autocorrelation	Arbitrary	ilr	-	-
Zaidi et al. ³⁹	T^2	AI with CC	Arbitrary	MLFFNN	-	-
Imran et al. ⁴⁰	T^2	AI with CC	p = 3, p = 5	MLPNN	-	-
Imran et al. ³⁷	VSI MEWMA	Addaptive	Arbitrary	ilr	FSI-MEWMA	VSI-MEWMA

Table 4: Summary of control chart for monitoring CoDa papers

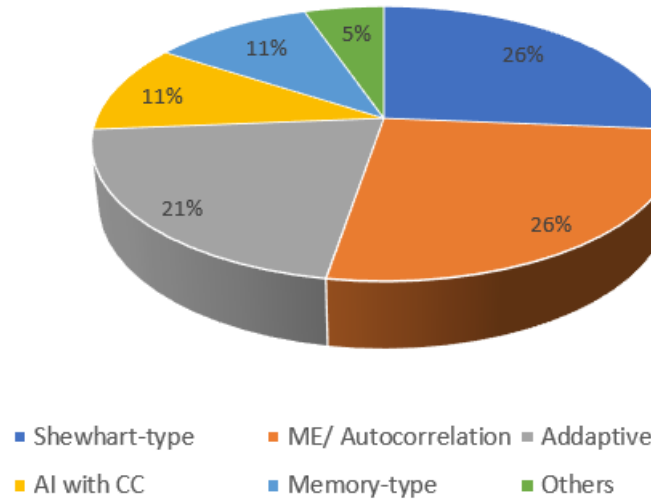


Figure 5: Cumulative number of papers over time

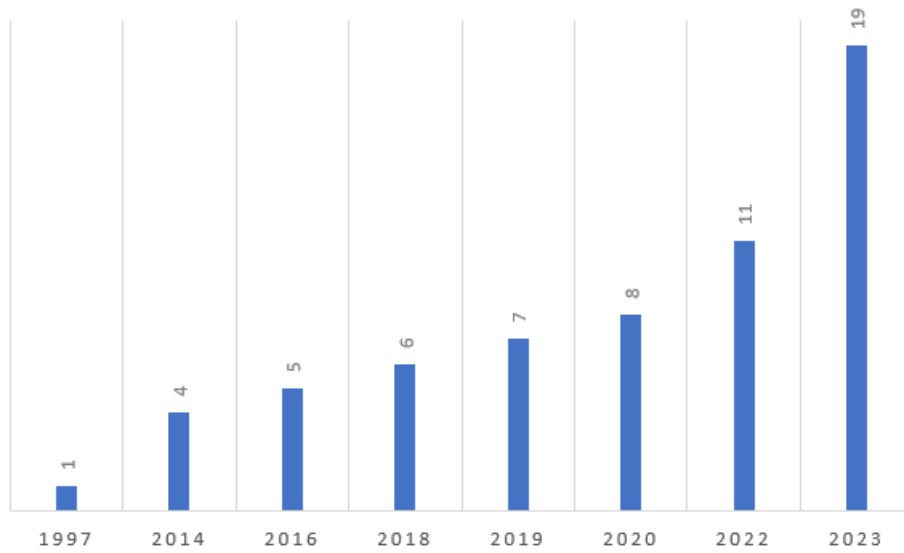


Figure 6: Cumulative number of papers over time

Figure 6 depicts the cumulative number of papers published from 1997 to 2023. It illustrates a significant upward trajectory in research related to monitoring CoDa, with a notably steep increase observed in 2023.

Table 5 presents the distribution of journals for the 19 papers reviewed in the field of monitoring CoDa. It is evident that “*Quality and Reliability Engineering International*” is at the forefront, with five papers (26.32%) of the total corpus, signifying its prominence as a platform for scholarly discourse in this field. Close behind is the “*Journal of Applied Statistics*”, hosting four papers (21.05%), which underscores its influential role in disseminating research findings. *Computers & Industrial Engineering* has two papers (10.53%) and other journals, each contributing one paper (5.26%), illustrating the

Journal	Number	Percentage
Quality and Reliability Engineering International	5	26.32%
Journal of Applied Statistics	4	21.05%
Computers & Industrial Engineering	2	10.53%
Revista Colombiana de Estadística	1	5.26%
Journal of Quality Technology	1	5.26%
IIE Transactions	1	5.26%
Journal of Statistical Computation and Simulation	1	5.26%
CMES-Computer Modeling in Engineering & Sciences	1	5.26%
Statistical Modelling	1	5.26%
IFAC-PapersOnLine	1	5.26%
Expert Systems with Applications	1	5.26%

Table 5: Number and percentage of papers in each journal

field’s interdisciplinary breadth. This spread across various journals indicates a wide interest in applications of CoDa analysis. The data denotes a vibrant academic ecosystem where multiple specialized journals serve as conduits for advancing the frontiers of monitoring CoDa research.

Table 6 provides a snapshot of the contributions made by various authors, presenting a clear disparity in the number of contributions among them. Fatima Sehar Zaidi emerges as the most prolific contributor, with a total of 11 contributions. Following closely is Muhammad Imran, with 9 contributions, and Kim Phuc Tran along with Jinsheng Sun, each with 7 contributions, showcasing their active participation. Other authors have made moderate contributions, ranging from 1 to 4 papers, indicating steady engagement in the field.

4 Perspectives for Monitoring the Ratio of Two Normal Variables and Compositional Data in the Industry 5.0

In this section, we will offer our perspective on applying existing ML methodologies in monitoring CoDa and the ratio of two normal random variables, and highlight potential areas for future research within the dynamic and evolving landscape of Industry 5.0. We place a special emphasis on the integration of ML techniques at various stages – from the design to the pattern recognition, and the interpretation of control charts. By dissecting the current trends and forecasting future developments, this section endeavors to provide valuable insights for researchers and practitioners alike, navigating the intricate intersection of statistical control processes and advanced technological paradigms.

Author	Number of contributions
Fatima Sehar Zaidi	11
Muhammad Imran	9
Kim Phuc Tran	7
Jinsheng Sun	7
Zameer Abbas	4
Hafiz Zafar Nazir	4
Marina Vives-Mestres	3
Josep Daunis-I-Estadella	3
Josep-Antoni Martín-Fernández	3
Philippe Castagliola	3
Michael Boon Chong Khoo	3
Xuelong Hu	3
Hong-Liang Dai	3
Anan Tang	2
Russell Boyles	1
Rubén Darío Guevara-González	1
José Alberto Vargas-Navas	1
Dorian Luis Linero-Segrera	1
Giovanni Celano	1
Thi Thuy Van Nguyen	1
Cédric Heuchenne	1
Christian H. Weiß	1

Table 6: Authors' contribution to the area of monitoring CoDa

4.1 Intergrating ML techniques in designing control charts

As stated before, autocorrelation is a common occurrence in real-life data, especially in industrial and manufacturing processes, where it significantly affects the integrity and interpretation of time-series data, making it a critical factor to consider in the design of control charts for monitoring CoDa. In response, advanced ML techniques present a formidable solution. For example, long short-term memory (LSTM) networks, as introduced by Schmidhuber et al.⁴¹, excel in capturing temporal dependencies, crucial for accurate data analysis in autocorrelated environments. Gaussian process regression (GPR), detailed by Williams and Rasmussen⁴², provides a powerful probabilistic approach, suitable for handling complex, interdependent variables in such data. Additionally, transformer models introduced in the paper “Attention is all you need” by Vaswani et al.⁴³ with their novel multihead attention mechanisms, are highly effective in identifying relevant sequential data patterns. The attention mechanisms in transformer models allow them to focus on specific parts of a data sequence that are most relevant for predictions. This feature is particularly useful in scenarios with autocorrelation, as it helps in identifying significant changes or trends within the data. Autoencoders (AE), recognized for anomaly detection and feature extraction, can distinguish between normal and aberrant patterns, especially valuable in cases of complex deviations due to autocorrelation. By integrating these advanced ML techniques with existing control chart methodologies, a more robust, accurate, and adaptive control chart can be designed. This integration not only enhances the accuracy and reliability of control charts but also ensures they are well-equipped to handle the complexities of modern industrial data, leading to improved monitoring, decision-making, and operational efficiency in various industrial applications.

As an example of such integration, in our forthcoming paper, titled “A novel transformer-based anomaly detection approach for ECG monitoring healthcare system”, we explored the integration of a Transformer-based variational AE with a MEWMA-Support vector data description (SVDD) control chart for the purpose of monitoring electrocardiogram (ECG) data. This innovative approach has demonstrated significant potential, yielding impressive results in terms of both accuracy and control of false alarm rates. The effectiveness of this method is particularly critical in healthcare settings, where precise and reliable monitoring is paramount, but it also holds substantial promise for various other fields that require precise data analysis and anomaly detection. This work exemplifies the advancements in leveraging sophisticated ML techniques to enhance the efficacy and reliability of monitoring systems in critical applications. Another example that can be mentioned is the work of Wang and Liu⁴⁴. In this work, the authors proposed a new control chart utilizing the isolation forest (iForest) algorithm, offering advantages such as lower computational complexity, superior performance in detecting small shifts in various distributions, and effectiveness in handling challenging distributions with heavy tails, suggesting its potential applicability in designing efficient control charts for monitoring CoDa.

Toward the control chart for monitoring the ratio of two normal variables, considering autocorrelation is also important. In this context, incorporating a bivariate first-order vector autoregressive (VAR(1)) model is a prudent choice. This model accounts for both autocorrelation and cross-correlation, which are prevalent in scenarios with high-frequency data collection. In Nguyen et al.⁴⁵, the authors exemplified this approach and showed that autocorrelation among observations adversely affects the performance of the Shewhart control chart for monitoring the ratio of two normal variables. For future research, it is important to consider the performance of other types of control charts, such as EWMA and CUSUM, for monitoring ratios in the presence of autocorrelation. Additionally, conducting research to design advanced control charts that can alleviate the adverse effects of autocorrelation is crucial for enhancing process monitoring effectiveness.

4.2 ML-based control charts pattern recognition for monitoring CoDa/Ratio

This perspective will be applied to both control charts used for monitoring CoDa and the ratio of two normal random variables, which, for brevity and clarity in our discussion, will henceforth be referred to as “CoDa/Ratio”.

The integration of ML techniques in Control Chart Pattern Recognition (CCPR) represents a transformative development in the field of SPC, including monitoring of CoDa/Ratio. In the 21st century, the rapid advancement of information technology and the proliferation of big data have catalyzed a significant shift in how control charts are interpreted and utilized. Historically, the interpretation of control charts relied heavily on heuristic rules, drawing largely on the experience and judgment of operators. This approach, while valuable, had its limitations, particularly in its dependence on human expertise and the potential for variability in interpretations. The emergence of expert systems marked a significant stride in addressing these limitations. These systems, which combine a set of expert-derived rules with data flows from the processes being controlled, represented an early form of automation in process monitoring. However, at the end of the 1980s, Neural Networks (NNs) began to be utilized for automating the reading and interpretation of control charts, as noted by Pugh⁴⁶. NN, as a form of ML, offers a more dynamic and adaptable approach compared to expert systems. They could learn directly from data, identify patterns, and make predictions or decisions without being explicitly programmed with the rules. This marked the beginning of the dominance of ML in pattern recognition, including CCPR.

ML algorithms have been shown to outperform traditional models in various practical situations. For instance, Guh⁴⁷ highlighted the capabilities of NN models in learning, self-organizing, and recognizing patterns from noisy or incomplete data representations – tasks that are challenging for human operators, even with the support of expert systems. Li et al.⁴⁸ proposed a Support Vector Machine (SVM)-based CCPR framework, demonstrating its superior accuracy in classifying the sources of out-of-control signals compared to conventional multivariate control schemes. Similarly, Diren et al.⁴⁹ reported that traditional CCPR models often fall short in predicting unexpected new situations, a gap effectively bridged by ML techniques. By learning from historical data, ML models can anticipate and adapt to new scenarios, enhancing the predictive capabilities of control charts. The evolving landscape of ML-based techniques CCPR brings a promising development for monitoring complex scenarios. For instance, SVM, since its introduction by Vapnik et al.⁵⁰, has been instrumental in CCPR. Their ability to classify data in a higher-dimensional space for linear separability enhances their applicability in recognizing complex control chart patterns, see, for example, Lin et al.⁵¹. Neural Networks (NNs) and Deep Learning have brought a new dimension to CCPR. The pioneering work of Pugh⁴⁶ and the subsequent advancements by researchers like Cheng⁵² and Addeh et al.⁵³ have highlighted the robust pattern recognition capabilities of these models. NNs’ adaptability in various conditions, including their effectiveness in environments with noise or incomplete data, positions them as powerful tools for intricate monitoring tasks. These ML techniques collectively represent a significant advancement in the field of CCPR, offering refined and accurate tools for analyzing complex data patterns. Their effectiveness across various monitoring scenarios underscores their potential to revolutionize process control and monitoring in industries requiring high precision and reliability.

The application of advanced ML techniques for CCPR, particularly for CoDa/Ratio, remains a largely unexplored area. There is a significant need for further research to develop methods using ML to effectively monitor these types of data. While existing studies have made strides in reducing assumptions about data distribution when designing ML-based control charts, there are still challenges, such as autocorrelation in data, which is often encountered in time series data collected from Internet of Things

(IoT) sensors, and industrial processes. Currently, in Zaidi et al.³⁹, a novel methodology is introduced for monitoring CoDa. This method integrates a multilayer feed-forward neural network with a T^2 control chart to enhance the detection of patterns within control charts. Demonstrated to be effective even amidst out-of-control conditions, its proficiency is corroborated through detailed simulations and analytical assessments. This advancement represents a significant stride in the development of ML techniques, challenging and potentially superseding the conventional assumptions embedded in traditional SPC. The efficiency and effectiveness offered by this novel approach underscore its potential in refining the monitoring of intricate data structures inherent in contemporary industrial processes. The direct future studies from this study can be the integration of MLFFNN with MEWMA, MCUSUM, and other advanced control charts (as mentioned in previous sections) for monitoring CoDa/Ratio.

For a comprehensive understanding of ML techniques in CCPR, one can refer to the detailed work of Tran et al.⁵⁴. In their study, the authors provide an in-depth summary and analysis of the field, offering valuable insights into the application and effectiveness of various ML approaches in enhancing CCPR.

4.3 Interpreting out-of-control signal for CoDa control charts

In this subsection, we will give our perspective exclusively on interpreting out-of-control signals in control charts for monitoring CoDa. This focused approach stems from the fact that the ratio of two normal variables is effectively managed using univariate control charts and has a well-established framework for signal interpretation. Given this established understanding, there is no pressing need to delve into the interpretation of out-of-control signals for this type of chart. Therefore, we will only concentrate on the more complex and nuanced realm of CoDa, where the interpretation of signals is required due to its multidimensional nature and the constraints it presents.

Interpreting out-of-control signals when monitoring CoDa presents a particular challenge, especially when considering the special structure of CoDa and the presence of autocorrelation in data in general. Traditional multivariate control charts, such as Hotelling's T^2 , MEWMA, and MCUSUM, for monitoring such data often only signal the general mean shifts without specifying the responsible variable(s). In general, some ML methods are being integrated into the process with promising results. NNs, SVM, decision trees, MLP, and DL have been explored to isolate and identify the specific causes of out-of-control conditions, see Niaki and Abbasi⁵⁵; Cheng and Cheng⁵⁶; Guh and Shiue⁵⁷, and Diren et al.⁴⁹ among many others for more information. These ML techniques not only offer a more precise identification of variables responsible for shifts but also improve upon the traditional charts' sensitivity to process anomalies. As these methods continue to evolve, they represent a significant potential in advancing the interpretability of control charts. These methods can be integrated into control charts for monitoring the ratio of two normal variables, however, due to the special structure of CoDa, these ML techniques can not be applied directly. Recently, there has been an attempt to interpret the out-of-control signals in CoDa monitoring by employing an NN technique in the work of³⁹. In this study, an MLPNN with back-propagation learning has been introduced to interpret signals within Hotelling's T^2 control chart specifically for CoDa monitoring processes. This approach helps in pinpointing the specific variables causing deviations, rather than merely indicating shifts in the overall mean. Such focused detection is crucial for refining process control strategies, ultimately improving the efficiency of industrial operations. The model's effectiveness was validated in scenarios involving different components of CoDa, $p = 3$ and $p = 5$. This innovation represents a significant step forward in applying ML to ensure the precision and reliability of process monitoring in industrial settings. Future research directions could consider the integration of MLPNN with MCUSUM or MEWMA CoDa control charts to increase adaptability. Additionally, merging MLPNN with clus-

tering algorithms or econometric models may offer new opportunities for innovation in the analysis of CoDa. Besides, the scarcity of robust methods for interpreting out-of-control signals in the monitoring of CoDa underscores a critical need for concentrated research efforts to develop new techniques in this field.

5 Conclusion

This chapter delivers an in-depth review and analysis of the methodologies for monitoring the ratio of two normal variables and CoDa within the Industry 5.0 framework. We began with a short introduction, setting the stage for the importance and challenges of CoDa/Ratio monitoring in industrial processes. Subsequently, we delved into an extensive examination of published research, analyzing 68 papers focused on monitoring the ratio of two normal variables and 19 dedicated to CoDa. In this exploration, we categorized the existing methodologies into relevant groups, offering a comprehensive analysis of these findings. This includes examining trends, assessing the distribution of publications across various journals, and highlighting the contributions of key authors in the field. Throughout each segment, we interjected our perspectives and insights, enriching the reader's understanding with deeper context and expert commentary on the results.

In our perspectives section, we offered insights on applying existing ML methodologies to CoDa and the ratio of two normal random variables. We stressed the importance of integrating ML techniques at various stages, from design to pattern recognition and interpretation of control charts. This perspective is essential for navigating the intersection of statistical control processes and advanced technological paradigms in Industry 5.0.

The paper concludes by emphasizing the need for ongoing research and development in this area. The integration of emerging technologies like AI and big data analytics with traditional monitoring methods promises further advancements in the field, potentially revolutionizing the efficacy and reliability of monitoring systems in smart manufacturing and Industry 5.0.

References

- [1] G. Celano, P. Castagliola, A. Faraz, and S. Fichera. Statistical Performance of a Control Chart for Individual Observations Monitoring the Ratio of two Normal Variables. *Quality and Reliability Engineering International*, 30(8):1361–1377, 2014.
- [2] J. Aitchison. *The Statistical Analysis of Compositional Data (Monographs on Statistics and Applied Probability)*. Chapman & Hall Ltd., London, (Reprinted in 2003 with additional material by The Blackburn Press), 1986.
- [3] D.C. Montgomery. *Statistical Quality Control: a Modern Introduction*. Wiley, New York, 2009.
- [4] G. Celano and P. Castagliola. Design of a Phase II Control Chart for Monitoring the Ratio of two Normal Variables. *Quality and Reliability Engineering International*, 32, 2014.
- [5] A.W. Spisak. A Control Chart for Ratios. *Journal of Quality Technology*, 22(1):34–37, 1990.
- [6] D. Oksoy, E. Boulos, and L.D. Pye. Statistical Process Control by the Quotient of two Correlated Normal Variables. *Quality Engineering*, 6(2):179–194, 1994.
- [7] G. Celano and P. Castagliola. A Synthetic Control Chart for Monitoring the Ratio of Two Normal Variables. *Quality and Reliability Engineering International*, 2015.

- [8] K.P. Tran, P. Castagliola, and G. Celano. Monitoring the ratio of two normal variables using Run Rules type control charts. *International Journal of Production Research*, ahead-of-print: 1–19, 2015.
- [9] Kim Phuc Tran, Philippe Castagliola, and G. Celano. Monitoring the ratio of two normal variables using ewma type control charts. *Quality and Reliability Engineering*, 10 2015.
- [10] Kim Phuc Tran and Sven Knoth. Steady-state arl analysis of arl-unbiased ewma-rz control chart monitoring the ratio of two normal variables. *Quality and Reliability Engineering*, 34, 11 2017.
- [11] Kim Phuc Tran, Philippe Castagliola, and G. Celano. Monitoring the ratio of population means of a bivariate normal distribution using cusum type control charts. *Statistical Papers*, 59, 03 2018.
- [12] Huu Du Nguyen, Kim Phuc Tran, and Thong Ngee Goh. Variable sampling interval control charts for monitoring the ratio of two normal variables. *Journal of Testing and Evaluation*, 48, 12 2019.
- [13] Huu Du Nguyen, Kim Phuc Tran, and Cédric Heuchenne. Monitoring the ratio of two normal variables using variable sampling interval exponentially weighted moving average control charts. *Quality and Reliability Engineering International*, 35(1):439–460, 2019.
- [14] Huu Du Nguyen, Kim Phuc Tran, and Henri L. Heuchenne. Cusum control charts with variable sampling interval for monitoring the ratio of two normal variables. *Quality and Reliability Engineering International*, 36(2):474–497, 2020.
- [15] Kim Phuc Tran, Philippe Castagliola, and G. Celano. The performance of the shewhart-rz control chart in the presence of measurement error. *International Journal of Production Research*, 54, 05 2016.
- [16] Huu-Du Nguyen and Kim Phuc Tran. Effect of the measurement errors on two one-sided shewhart control charts for monitoring the ratio of two normal variables. *Quality and Reliability Engineering International*, 36, 05 2020.
- [17] H.D. Nguyen, K.P. Tran, and K.D. Tran. The effect of measurement errors on the performance of the Exponentially Weighted Moving Average control charts for the Ratio of Two Normally Distributed Variables. *European Journal of Operational Research*, 293(1):203–218, 2021.
- [18] Sani Salihu Abubakar, Michael B. C. Khoo, Sajal Saha, Adamu Abubakar Umar, and Wai Chung Yeong. Run sum ratio chart when measurement errors are present. *Quality and Reliability Engineering International*, 38(8):4049–4072, 2022.
- [19] V. Pawlowsky-Glahn, J. J. Egozcue, and R. Tolosana-Delgado. *Modeling and Analysis of Compositional Data*. John Wiley & Sons, 2015.
- [20] J. J. Egozcue, V. Pawlowsky-Glahn, G. Mateu-Figueras, and C. Barceló-Vidal. Isometric logratio transformations for compositional data analysis. *Mathematical Geology*, 35(3):279–300, 2003.
- [21] J.J. Egozcue and V. Pawlowsky-Glahn. Groups of Parts and Their Balances in Compositional Data analysis. *Mathematical Geology*, 37(7):795–828, 2005.
- [22] R. A. Boyles. Using the chi-square statistic to monitor compositional process data. *Journal of Applied Statistics*, 24(5):589–602, 1997.
- [23] R. Guevara, J. Vargas, and D. Linero Segrera. Profile monitoring for compositional data. *Revista Colombiana de Estadística*, 37:159, 07 2014.

- [24] M. Vives-Mestres, J. Daunis-I-Estadella, and J.A. Martin-Fernandez. Out-of-Control Signals in Three-Part Compositional T^2 Control Chart. *Quality and Reliability Engineering International*, 30(3):337–346, 2014.
- [25] M. Vives-Mestres, J. Daunis-I-Estadella, and J.A. Martin-Fernandez. Individual T^2 Control Chart for Compositional Data. *Journal of Quality Technology*, 46(2):127–139, 2014.
- [26] K. P. Tran, P. Castagliola, G. Celano, and Michael B.C. Khoo. Monitoring compositional data using multivariate exponentially weighted moving average scheme. *Quality and Reliability Engineering International*, 34(3):391–402, 2018.
- [27] M. Imran, J. Sun, F.S. Zaidi, Z. Abbas, and H.Z. Nazir. Multivariate cumulative sum control chart for compositional data with known and estimated process parameters. *Quality and reliability engineering international*, 38(5), 2022-07. ISSN 0748-8017.
- [28] T.T.V. Nguyen, C. Heuchenne, and K.P. Tran. Anomaly detection for compositional data using vsi mewma control chart. *IFAC-PapersOnLine*, 55(10):1533–1538, 2022. ISSN 2405-8963. 10th IFAC Conference on Manufacturing Modelling, Management and Control MIM 2022.
- [29] M. Imran, J. Sun, F.S. Zaidi, Z. Abbas, and H.Z. Nazir. On designing efficient multivariate exponentially weighted moving average control chart for compositional data using variable sample size. *Journal of Statistical Computation and Simulation*, 93(10):1622–1643, 2023.
- [30] C.A. Lowry, W.H. Woodall, C.W. Champ, and S.E. Rigdon. A Multivariate Exponentially Weighted Moving Average Control Chart. *Technometrics*, 34(1):pp. 46–53, 1992. ISSN 00401706.
- [31] F.S. Zaidi, P. Castagliola, K.P. Tran, and M.B.C. Khoo. Performance of the hotelling t_2 control chart for compositional data in the presence of measurement errors. *Journal of Applied Statistics*, 46(14):2583–2602, 2019.
- [32] F.S. Zaidi, P.Y. Castagliola, K.P. Tran, and M.B.C. Khoo. Performance of the mewma-coda control chart in the presence of measurement errors. *Quality and Reliability Engineering International*, 36(7):2411–2440, 2020.
- [33] M. Imran, J. Sun, F.S. Zaidi, Z. Abbas, and H.Z. Nazir. Effect of measurement error on the multivariate cusum control chart for compositional data. *CMES-Computer Modeling in Engineering & Sciences*, 136(2), 2023.
- [34] M. Imran, J. Sun, F.S. Zaidi, Z. Abbas, and H.Z. Nazir. Evaluating the performance of variable sampling interval hotelling t_2 charting scheme for compositional data in the presence of measurement error. *Quality and Reliability Engineering International*, 2023.
- [35] F.S. Zaidi, H.L. Dai, M. Imran, and K.P. Tran. Monitoring autocorrelated compositional data vectors using an enhanced residuals hotelling t_2 control chart. *Computers & Industrial Engineering*, 181:109280, 2023.
- [36] M. Vives-Mestres, J. Daunis-i Estadella, and J. A. Martin-Fernandez. Signal interpretation in hotelling’s t_2 control chart for compositional data. *IIE Transactions*, 48(7):661–672, 2016.
- [37] M. Imran, J. Sun, X. Hu, F.S. Zaidi, and A. Tang. Investigating zero-state and steady-state performance of mewma-coda control chart using variable sampling interval. *Journal of Applied Statistics*, pages 1–22, 2023.
- [38] C.H. Weiß. Ordinal compositional data and time series. *Statistical Modelling*, page 1471082X231190971, 2023.

- [39] F.S. Zaidi, H.L. Dai, M. Imran, and K.P. Tran. Analyzing abnormal pattern of hotelling t2 control chart for compositional data using artificial neural networks. *Computers & Industrial Engineering*, 180:109254, 2023.
- [40] M. Imran, H.L. Dai, F.S. Zaidi, X. Hu, K.P. Tran, and J. Sun. Analyzing out-of-control signals of t2 control chart for compositional data using artificial neural networks. *Expert Systems with Applications*, page 122165, 2023.
- [41] J. Schmidhuber, S. Hochreiter, et al. Long short-term memory. *Neural Comput*, 9(8):1735–1780, 1997.
- [42] C.K.I. Williams and C.E. Rasmussen. *Gaussian processes for machine learning*, volume 2. MIT press Cambridge, MA, 2006.
- [43] A. Vaswani, N. Shazeer, N. Parmar, J. Uszkoreit, L. Jones, A.N. Gomez, L. Kaiser, and I. Polosukhin. Attention is all you need. *Advances in neural information processing systems*, 30, 2017.
- [44] J. Wang and L. Liu. A new multivariate control chart based on the isolation forest algorithm. *Quality Engineering*, pages 1–17, 2023.
- [45] H.D. Nguyen, A.A. Nadi, K.D. Tran, P. Castagliola, G. Celano, and K.P. Tran. The shewhart-type rz control chart for monitoring the ratio of autocorrelated variables. *International Journal of Production Research*, 61(20):6746–6771, 2023.
- [46] G.A. Pugh. Synthetic neural networks for process control. *Computers & industrial engineering*, 17(1-4):24–26, 1989.
- [47] R.S. Guh. Real-time recognition of control chart patterns in autocorrelated processes using a learning vector quantization network-based approach. *International Journal of Production Research*, 46(14):3959–3991, 2008.
- [48] T. Li, S. Hu, Z.Y. Wei, Z.Q. Liao, et al. A framework for diagnosing the out-of-control signals in multivariate process using optimized support vector machines. *Mathematical Problems in Engineering*, 2013, 2013.
- [49] D.D. Diren, S. Boran, and I. Cil. Integration of machine learning techniques and control charts in multivariate processes. 2020.
- [50] V. Vapnik, I. Guyon, and T. Hastie. Support vector machines. *Machine Learning*, 20(3):273–297, 1995.
- [51] S.Y. Lin, R.S. Guh, and Y.R. Shiue. Effective recognition of control chart patterns in autocorrelated data using a support vector machine based approach. *Computers & Industrial Engineering*, 61(4):1123–1134, 2011.
- [52] C.S. Cheng. A neural network approach for the analysis of control chart patterns. *International Journal of Production Research*, 35(3):667–697, 1997.
- [53] A. Addeh, A. Khormali, and N.A. Golilarz. Control chart pattern recognition using rbf neural network with new training algorithm and practical features. *ISA transactions*, 79:202–216, 2018.
- [54] P.H. Tran, A. Ahmadi Nadi, T.H. Nguyen, K.D. Tran, and K.P. Tran. Application of machine learning in statistical process control charts: A survey and perspective. In *Control charts and machine learning for anomaly detection in manufacturing*, pages 7–42. Springer, 2022.

- [55] S.T.A. Niaki and B. Abbasi. Fault diagnosis in multivariate control charts using artificial neural networks. *Quality and reliability engineering international*, 21(8):825–840, 2005.
- [56] C.S. Cheng and H.P. Cheng. Identifying the source of variance shifts in the multivariate process using neural networks and support vector machines. *Expert Systems with Applications*, 35(1-2): 198–206, 2008.
- [57] R.S. Guh and Y.R. Shiue. An effective application of decision tree learning for on-line detection of mean shifts in multivariate control charts. *Computers & Industrial Engineering*, 55(2):475–493, 2008.